HHS Public Access

Author manuscript

Curr Biol. Author manuscript; available in PMC 2016 March 16.

Published in final edited form as:

Curr Biol. 2015 March 16; 25(6): 713–721. doi:10.1016/j.cub.2015.01.024.

Ocular dominance plasticity disrupts binocular inhibition-excitation matching in visual cortex

M. Hadi Saiepour[1], **Rajeev Rajendran**[1], **Azar Omrani**[1], **Wen-pei Ma**[2], **Huizhong W. Tao**[2], **J. Alexander Heimel**[1], and **Christiaan N. Levelt**[1,*]

[1] Department of Molecular Visual Plasticity, The Netherlands Institute for Neuroscience, Royal Netherlands Academy of Arts and Sciences (KNAW), Meibergdreef 47, 1105 BA Amsterdam, the Netherlands [2] Zilkha Neurogenetic Institute, Department of Cell & Neurobiology, University of Southern California, 1501 San Pablo St. ZNI 439, Los Angeles, CA 90033, USA

Abstract

Background—To ensure that neuronal networks function in a stable fashion, neurons receive balanced inhibitory and excitatory inputs. In various brain regions this balance has been found to change temporarily during plasticity. Whether changes in inhibition have an instructive or permissive role in plasticity remains unclear. Several studies have addressed this question using ocular dominance plasticity in the visual cortex as a model, but so far it remains controversial whether changes in inhibition drive this form of plasticity by directly affecting eye-specific responses or through increasing the plasticity potential of excitatory connections.

Results—We tested how three major classes of interneurons affect eye-specific responses in normally reared or monocularly deprived mice by optogenetically suppressing their activity. We find that in contrast to somatostatin or vasoactive intestinal polypeptide expressing interneurons, parvalbumin (PV)-expressing interneurons strongly inhibit visual responses. In individual neurons of normal mice, inhibition and excitation driven by either eye are balanced and suppressing PV interneurons does not alter ocular preference. Monocular deprivation disrupts the binocular balance of inhibition and excitation in individual neurons, causing suppression of PV interneurons to change their ocular preference. Importantly however, these changes do not consistently favor responses to one of the eyes at the population level.

Conclusion—Monocular deprivation disrupts the binocular balance of inhibition and excitation of individual cells. This disbalance does not affect the overall expression of ocular dominance. Our data therefore support a permissive rather than an instructive role of inhibition in ocular dominance plasticity.

* Correspondence: Christiaan N. Levelt, Netherlands Institute for Neuroscience, Meibergdreef 47, 1105 BA Amsterdam, the Netherlands. Tel: +31205665359. c.levelt@nin.knaw.nl.

Introduction

Neuronal responses are formed by interactions between excitatory and inhibitory inputs, which are typically well-balanced. This balance between inhibition and excitation is believed to be important for maintaining the stability of neuronal networks and increasing their dynamic range [1,2]. At the single neuron level, inhibition and excitation are often tuned to the same features of stimuli, thus ensuring that excitatory inputs are rapidly and specifically inhibited [3,4]. Such co-tuning of inhibition and excitation is well-described for sound frequency tuning in auditory cortex [5] where it improves the temporal precision of neuronal responses. Inhibition is also tuned to excitation during orientation tuning in primary visual cortex (V1) where it mediates contrast-independent orientation tuning [6]. The balance of inhibition and excitation is also important for regulating cortical plasticity [7,8]. Recent reports found that a decrease in the inhibition:excitation ratio occurs at the onset of plasticity. This was observed during ocular dominance (OD) plasticity in V1 [9-11], watermaze learning in the hippocampus [12], retuning of sound frequency preference in the auditory cortex [13] and whisker deprivation in the somatosensory cortex [14]. While it has been shown that the initial decrease in inhibition is essential for triggering plasticity, it remains unclear how changes in inhibition contribute to plasticity and how inhibition readjusts afterwards.

Experiments in auditory cortex suggest that inhibition is reduced to enhance the plasticity potential of excitatory connections, after which inhibition readjusts to match the altered excitatory inputs [13]. But it has also been suggested that plasticity of inhibition may directly alter the responses of excitatory neurons by selectively disinhibiting preferred inputs and/or suppressing non-preferred inputs [15-17]. This mechanism has been observed in the inferior colliculus of the barn owl, where experience dependent changes in the auditory map of space involves selective inhibition of the normal map [18]. OD plasticity in V1 is a highly suitable model to distinguish between these scenarios. Temporary closure of one eye causes neurons in V1 to become more responsive to the open eye [19], a process which is associated with the plasticity of inhibitory innervation [9-11,20,21]. Unfortunately, experiments aimed at understanding how changes in inhibitory connectivity contribute to OD plasticity have provided conflicting results [22]. Some studies showed that interneurons and their inhibitory inputs onto excitatory neurons shift towards the non-deprived eye [23,24], favoring the idea that inhibition and excitation are binocularly balanced and maintain or regain this balance after OD plasticity. In contrast, other studies favored a scenario where plasticity of inhibitory connections directly affects the ocular preference of excitatory neurons [15,16], which could in part be achieved by an initial shift of the responsiveness of interneurons towards the deprived eye [17].

A possible cause of these apparent discrepancies is the diversity of cortical interneurons, which may differentially inhibit eye-specific responses of excitatory neurons. In this study we therefore tested how different interneuron subsets affect eye-specific responses by optogenetically suppressing their activity. If a specific subset of interneurons contributes to the expression of OD by preferentially inhibiting responses to one of the eyes, releasing this inhibition is expected to cause a relative increase in the responses to this eye.

We find that parvalbumin (PV) expressing interneurons, but not somatostatin (SST) or vasoactive intestinal peptide (VIP) expressing interneurons, provide strong inhibitory inputs during monocular visual stimulation. In undeprived mice, these inhibitory inputs are matched to excitatory inputs from each of the two eyes down to the level of individual neurons. Monocular deprivation (MD) disrupts this binocular balance of inhibition and excitation. While this causes inhibitory inputs to alter the ocular preference of individual neurons, this change does not consistently favor one eye and does not contribute to the altered expression of ocular dominance at the population level.

Results

Suppressive effects of different interneuron subsets on cortical responses

Our first aim was to assess the contribution of different interneuron subsets to visual responses in V1 during the critical period for OD plasticity. To this end we optogenetically suppressed the activity of PV-, SST- and VIP-expressing interneurons in V1 by making use of the light-activated proton pump archaerhodopsin (Arch) [25]. These three non-overlapping interneuron subsets represent 85% of all cortical interneurons. Neurogliaform interneurons, which provide less specific volume release of GABA, are not included in these subsets. An AAV vector driving Arch expression in a cre-dependent fashion was injected into the visual cortex of 3-5 day old mice expressing cre-recombinase specifically in the relevant interneuron subsets (Fig. 1A). This resulted in highly specific and widespread expression of Arch-GFP in the targeted subsets of interneurons by the time the mice were 4-5 weeks old (Fig. 1B). Fluorescent microscopy through the skull was employed to validate that Arch-GFP expression covered the entire binocular region of V1 before the onset of single unit recordings. Post-hoc immunohistochemical analyses showed that 79-94% of interneurons in the targeted area expressed Arch-GFP (Fig 1C-D).

Mice were either reared normally, or monocularly deprived for 7 days. Responses of single units in V1 to visual stimuli presented monocularly to both eyes were recorded while interneurons were intermittently suppressed when the mice were 34-36 days old (Fig. 1A). When mice were monocularly deprived for shorter periods, single unit recordings took place earlier (p29-p32). The experiments were performed in lightly anesthetized animals, allowing the direct comparison of our findings with previous studies in which the contribution of inhibition to the expression of ocular dominance plasticity was investigated. We aimed to moderately reduce inhibition in order to stay within a physiological range [26] and minimize saturation of responses. The latter is important, as saturation may cause a decrease in the differences between contra- and ipsilateral responses making neurons appear more binocular. Arch-mediated suppression of PV+ interneurons increased average responses of single units by 25% (normalized firing rate: 1.25±0.04, n=56 from 9 mice, Wilcoxon signed-rank test $p<0.0001$) (Fig. 2A) and responsiveness did not cause saturation of responses at any contrast (Fig. 2B-C, Fig. S1A, B). Increasing optogenetic suppression further strengthened the firing rates of neurons in V1 (high light, normalized firing rate 1.67±0.19, n=22 from 4 mice, Wilcoxon signed-rank test, $p<0.05$ vs low light) thus confirming that responses were not saturated (Fig. 2B). Suppression of PV+ interneurons significantly changed the contrast response curves of most neurons in V1 throughout all cortical depths

(for examples, see Fig. S1 and Fig. 2D, depicting a strongly modulating neuron) and caused 71.9% of all neurons to increase their firing rates (Fig. 2G). This resulted in the average contrast response curve to shift upward (Fig. 2C) [27-30], although some neurons showed a multiplicative increase in responsiveness upon suppression of PV+ interneurons (Fig. S1) [26,31]. Surprisingly, in mice expressing Arch in SST+ or VIP+ interneurons (Fig. 2A) we did not find a change in the average responsiveness of cortical neurons although up to three times more light was applied (SST: 0.94±0.04, n=27 cells, Wilcoxon signed-rank test, p=0.07, 9 mice, VIP: 1.02±0.03, n=19 cells, p=0.87, 5 mice). Much fewer neurons showed a significant change in their contrast tuning curves upon suppression of SST+ or VIP+ interneuron (Fig. 2E, F, H, I) and the response change was generally weak. Upon optogenetic suppression of SST+ interneurons, 9.1% of neurons showed slightly increased responses and 18.2% responded more weakly (Fig. 2H). About half of these neurons showed strongly reduced responses and possibly represented SST+ interneurons that were optogenetically silenced (see example in Fig. 2E, Fig. S1). Upon optogenetic suppression of VIP+ interneurons, 19.1% of neurons very mildly increased their responses (Fig. 2I, see Fig. 2F depicting the contrast-tuning curve of the most strongly modulated neuron), while 4.3% were slightly less active. To better understand the weak effects of suppressing SST+ and VIP+ interneurons, we assessed whether they were visually responsive under our experimental conditions and whether Arch-mediated suppression of their activity was effective. We performed two-photon imaging of calcium signals upon expressing the genetically encoded calcium sensor GCaMP6s [32] specifically in PV+, SST+ or VIP+ interneurons in juvenile mice (p33-p37). This revealed that all interneuron subsets showed clear calcium responses (Fig. 3A-C) and that slightly fewer SST+ and VIP+ interneurons in V1 were visually responsive compared to PV+ interneurons (Fig. 3D). We also assessed whether Arch-mediated suppression was effective in SST+ and VIP+ interneurons using cell-attached recordings, and found that this was indeed the case (Fig. 3E,F)(SST: light off/on 5.99±2.04Hz vs 0.02±0.01Hz, n=5 from 4 mice, Wilcoxon signed-rank, p=0.031, VIP: light off/on: 2.27±0.56 to 0.26±0.14, n=6 from 3 mice, p=0.016). Thus, VIP+ and SST + interneurons are visually responsive and their activity can be optogenetically modulated. However, optogenetic suppression of these interneuron subtypes only weakly changes the visual responses of few neurons in V1 under conditions for OD assessment. Possibly, additional modulatory inputs are required in order for SST+ and VIP+ interneurons to effectively alter cortical responses, as previously observed in awake animals[33,34].

Reducing PV+ interneuron mediated inhibition does not alter the OD index of population responses in normally reared or monocularly deprived mice

Having identified PV+ interneurons as the main inhibitory input, we asked whether they contributed to the ocular dominance index (ODI) of the population response in normally reared mice. We found that suppressing PV+ interneurons did not cause a larger change in the population ODI than shining light on V1 of mice expressing GFP in PV+ interneurons (Fig. 4A) (GFP in PV+ interneurons:ΔODI light off/on: 0.092±0.054, n=11 from 3 mice vs Arch in PV+ interneuronsΔODI light off/on: 0.047±0.032, n=42 from 7 mice, Dunnett's test, p=0.94).

Because previous studies have observed that inhibitory innervation is altered during OD plasticity we asked whether PV+ interneurons influenced the population ODI after a period of MD. When mice were monocularly deprived for 3-4 or 7 days, a strong OD shift was induced (Welch ANOVA, $F_{(3)}$=8.4, P<0.001, followed by Dunnett's test: no MD light off: 0.54±0.05, n=42 cells from 9 mice, vs 3-4d MD light off: 0.11±0.10, n=41 cells from 9 mice, p<0.001; 7d MD: 0.16±0.07 light off, n=42 cells from 7 mice, p<0.01), while the shift after 1 day MD (0.33±0.10, n=10, cells from 3 mice, p=0.70) was not significant (Fig. 4A). Optogenetic suppression of PV+ interneuron activity did not cause a change in the measured population ODI at any of these days (Welch ANOVA, $F_{(4)}$=0.51, p=0.72, GFP in PV+ interneuronsΔODI light off/on: 0.092±0.054, no MD: 0.047±0.032, 1d MD:ΔODI=0.026±0.04, 3-4d MD: ΔODI=0.054±0.024, 7d MD: ΔODI=0.003±0.051) (Fig. 4A) indicating that neither at the start nor after full induction, the OD shift can be attributed to a decrease or increase of inhibition of ipsi- or contralateral eye-specific responses respectively. As expected from their weak influence on visually driven responses in V1, suppression of SST+ and VIP+ interneurons also did not alter the population ODI in control mice or mice that were monocularly deprived for 7 days (Fig. S2A, B). These findings thus support the notion that the population ODI and its shift after MD are mainly determined by changes to thalamocortical and intracortical excitatory synapses [19,22,35].

Binocular matching of inhibition and excitation is disrupted by monocular deprivation

Although suppressing PV+ interneurons did not alter the population ODI it was possible that inhibitory inputs did affect the ODI of individual neurons. We therefore tested whether suppression of PV+ interneurons altered the ODI of neurons in V1 of normally reared mice. The scatter plot in figure 4B shows the ODI's of single units under normal conditions versus the ODI's of the same units upon optogenetic suppression of PV+ interneurons. In order to quantify whether PV+ interneurons significantly affected the ODI of individual neurons, we assessed the absolute change in the ODI of all units caused by suppressing PV+ interneurons and compared it to the absolute change observed upon shining light on V1 of mice expressing GFP in PV+ interneurons. This revealed that the ODI of individual neurons was not altered by suppressing PV+ interneurons (GFP: 0.13±0.05, n=11 from 3 mice vs Arch-no MD: 0.15±0.02, n=42 from 9 mice, t-test, sqrt transformation p=0.53) (Fig. 4F). This observation implies that inhibition and excitation of individual neurons are matched for inputs from either eye, otherwise reducing inhibition would be expected to change the relative response strength of the neuron to the two eyes. Indeed, whole cell recordings have previously shown that the ODI of inhibitory and excitatory conductances in each cell are correlated [36,37], see Fig. 4C (r=0.82, n=21 cells from 21 mice, chi-squared test, p<0.001).

Importantly, however, this situation changed notably after a week of MD. When the ODI's of single units from 7 day deprived mice were plotted against the ODI's of the same units during optogenetic suppression of PV+ interneurons, we observed that the values now deviated more strongly from the identity line (Fig. 4D). This was reflected in an increase in the absolute change in the ODI's of single units upon suppression of PV+ interneurons (Arch-no MD: 0.15±0.02, n=42 cells from 9 mice vs Arch-7d MD: 0.24±0.03, n=42 from 7 mice, Welch ANOVA, sqrt transformation, $F_{(3)}$=3.87, p=0.015, followed by Dunnett's test, p=0.042) (Fig. 4F). Monocular deprivation thus appeared to cause a disruption of the

binocular matching of inhibition and excitation on the single neuron level. To test this, we analyzed the correlation between the ODI values of inhibitory and excitatory conductances in single neurons as assessed by whole cell recordings in mice that were monocularly deprived for 6 days (data from [36] and additional recordings). As expected, this correlation was strongly reduced after MD (r=0.03, n=17 cells from 17 mice, p=0.92, and significantly lower than r=0.82 in non-deprived mice, Fisher r-to-z transformation $P<0.05$) (Fig. 4E). The absolute difference in the ODI between inhibitory and excitatory conductances had also increased (control: 0.090 to MD: 0.166, t-test, sqrt transformation, p=0.044) (Fig. 4G). Optogenetic suppression of SST+ or VIP+ interneurons did not alter the ODI of individual neurons in control mice or after 7 days of monocular deprivation (Fig. S2C, D). Together these findings show that inhibition and excitation are binocularly balanced in normally reared mice, and that monocular deprivation disrupts this balance. This loss of balanced inhibition and excitation causes the ODI of individual neurons to change upon optogenetic suppression of PV+ interneurons, but not upon suppression of SST+ or VIP+ interneurons.

Finally, we assessed whether the change in ODI of single units induced by suppression of PV+ interneurons as observed after 7 days of MD compared to non-deprived mice (Fig. 4F), could be observed after shorter periods of deprivation. We found that it did not yet occur at 1 or 3-4 days of MD (absolute change of ODI in undeprived mice: 0.15±0.02, n=42 from 9 mice vs 1d MD 0.095±0.024, n=10 cells from 3 mice, Dunnett's test, p=0.83; 3-4d MD: 0.12±0.02, n=41 cells from 9 mice, p=0.87). Thus, the change in ODI of individual neurons mediated by suppressing PV+ interneurons does not occur before or at the onset of the OD shift, but only several days after OD plasticity. The loss of binocularly matched inhibition and excitation therefore appears to be a consequence of OD plasticity.

Discussion

Here we show for the first time that under conditions typically used to assess OD in V1, PV + interneurons exert strong inhibitory control over cortical responses while SST+ and VIP+ interneurons hardly exert any. Furthermore we find that acutely reducing PV+ interneuron-mediated inhibition by optogenetics does not affect the expression of OD in neurons in V1. This is explained by our observation that the ocular preferences of inhibitory and excitatory inputs to individual neurons in V1 are highly correlated. This indicates that also when seeing with only one of the eyes, inhibition and excitation are balanced in binocular V1. Therefore, reducing inhibition affects responses to both eyes to a similar degree. It thus appears that under normal circumstances the expression of OD is mainly determined by excitatory connectivity [35].

Interestingly, one week of monocular deprivation drastically changes this situation and causes the ocular preference of inhibitory and excitatory inputs of neurons in V1 to diverge. As a consequence, optogenetic suppression of PV+ interneurons now changes the OD of individual excitatory neurons. This loss of binocular matching of inhibition and excitation may well underlie previous observations that the OD of individual neurons changes when inhibitory inputs are suppressed in monocularly deprived cats or mice [15-17]. It appears that this loss of binocularly matched inhibition and excitation is a late consequence of OD plasticity. Three days of monocular deprivation causes a strong OD shift, but suppressing

PV+ interneurons does not yet affect the OD of neurons in V1. A possible underlying mechanism may be that inhibitory and excitatory neurons undergo OD plasticity independently from each other and at different rates [17,23,24]. This is likely to disrupt the network mediating the binocularly matched inhibition and excitation unless a rapid and precise reorganization of inhibitory innervation would reestablish the balance.

Importantly, these findings do not imply that plasticity of inhibitory innervation selectively suppresses deprived eye responses or disinhibits open eye responses. The changes in the OD of individual neurons observed upon suppressing PV+ interneurons are not consistently biased towards one of the eyes. Instead, some neurons become more responsive to the deprived eye and others towards the non-deprived eye, leaving the OD of the total population unaffected. Because the changes in the ODI of individual neurons can clearly be observed, it seems unlikely that the moderate level of suppression of PV+ interneurons causes the lack of effect on the population response. We can however not rule out the possibility that further subdivision of PV+ cells would reveal interneurons that do influence eye-specific responses. Their effects may be masked by the broad suppression of more dominant and less specific types of PV+ interneurons or by the recurrent interactions between excitatory and inhibitory neurons. Making use of cre/flippase dual-recombinase systems may allow the genetic dissection of such cell types in the near future.

If plasticity of inhibitory innervation does not directly affect the expression of the OD shift, how does it contribute to OD plasticity? The previously observed decrease in inhibition at the onset of OD plasticity may augment the plasticity potential of excitatory connections. This could involve reduced stringency of spike-timing-dependent plasticity [38], or changes in the filtering of sensory inputs that drive cortical plasticity [39]. In auditory cortex, induction of plasticity by pairing an auditory stimulus with nucleus basalis stimulation also causes an initial reduction of inhibition [13]. Subsequently the inhibitory inputs follow the plasticity of excitatory inputs and become tuned to the same stimulus. It is unclear why inhibition and excitation do not rebalance in V1 after OD plasticity. Possibly, retuning of inhibition only occurs after reopening of the deprived eye. Alternatively, retuning does not occur at all after OD plasticity and may contribute to the visual deficits observed in amblyopia.

We found that during the assessment of OD, suppressing the activity of SST+ or VIP+ interneurons in V1 has little effect. Only few neurons change their responses to visual stimuli and their ODI's are not altered. SST+ interneurons, which mostly represent Martinotti cells, are sparser and show more selective and weaker responses than PV+ interneurons, especially under anesthesia [40]. In line with this, our calcium imaging experiments revealed that more PV+ interneurons than SST+ interneurons are visually responsive. In addition, SST+ interneurons predominantly innervate distal dendrites of pyramidal neurons in layer 1 [41], which receive associative inputs from other cortical areas and non-sensory thalamic nuclei [42]. These inputs may be more relevant in awake animals [43]. Together, these properties might explain why SST+ interneurons do not reduce the strong responses in V1 elicited by feedforward inputs from the two eyes. VIP+ interneurons in V1 were recently found to act predominantly by inhibiting SST+ interneurons [44]. In addition, running [34] and modulatory inputs [45] strongly modulate the activity of VIP+

interneurons. The weak effects of VIP+ silencing on visual responses may thus be caused by relatively weak activity of these cells under the conditions typically used for assessing OD, or an indirect effect of the absence of detectable SST+ interneuron-mediated inhibition in our experiments.

The observation that suppressing SST+ or VIP+ interneurons does not affect eye-specific responses suggests that previously observed consequences of blocking $GABA_A$-receptor-mediated inhibition on OD under comparable experimental conditions did not involve significant inputs from these interneuron subsets. In addition, this finding shows that the shift in OD is expressed in the absence of a direct contribution of SST+ or VIP+ interneurons to eye-specific responses. This does however not contradict the possibility that these interneuron subsets may contribute to OD plasticity by modulating cortical responses during the period of monocular deprivation [46].

It has recently been suggested that a developmental increase in subtractive inhibition by PV + interneurons suppresses spontaneous activity more strongly than visually driven activity [47]. This may open the critical period of OD plasticity by switching learning cues from internal to external sources. Our results confirm that suppressing PV+ interneuron mediated inhibition during the critical period results in an increase in spontaneous activity. It is interesting to speculate that further increases in PV+ interneuron may close the critical period by also suppressing weak visually driven responses. In adulthood, disinhibitory circuits activated by modulatory inputs may become essential for unmasking these inputs and allowing plasticity to occur.

Experimental procedures

Experimental animals

All animal experiments were approved by the institutional animal care and use committees of the Royal Netherlands Academy of Arts and Sciences, and University of Southern California. Procedures are elaborated in the Supplemental experimental procedures. To target populations of parvalbumin (PV), somatostatin (SST) and vasoactive intestinal polypeptide (VIP) expressing interneurons, respective cre-lines (Jackson Laboratories, www.jaxmice.org) were used.

Virus injection

Cre-dependent adeno-associated viral vectors (AAV) driving expression of archaerhodopsin-GFP (AAV-Arch) [25] or GCaMP6s (AAV-GCaMP6s) [32] were injected in PV-cre, SST-cre or VIP-cre mouse lines. Under isoflurane anesthesia, postnatal day 3-5 (P3-P5) pups were injected with AAV-Arch in the left primary visual cortex (V1) at a depth of 1.7 and 1.5 mm below the scalp surface.

Monocular deprivation

Right eyelids were sutured under isoflurane anesthesia between P27-P29. Eyes were reopened after 1-7 days and only mice with clear corneas were included for single unit recordings.

Single unit recordings and optogenetics

At P30-37, animals were anesthetized with Urethane (1g/kg, *i.p.*, Sigma-Aldrich) and Chlorprothixene (6.5mg/kg, *s.c.*, Sigma-Aldrich). Single unit and local field potential recordings were measured in layers 2-5 through a V1 craniotomy, using a tungsten in glass electrode (1MΩ, Alpha-Omega). An optical fiber (960μm diameter, NA=0.5) coupled to an amber (peak 595nm, Doric Lenses) LED light source was positioned such that the area of illumination was restricted to V1, and centered on the recording site. Visual stimuli including square flashes and square wave gratings were presented to check the receptive field and orientation tuning of single units, respectively. For optogenetic modulation, amber light was applied in an interleaved manner. Contrast sensitivity was measured by presenting gratings of various contrasts (0, 20, 40, 60, 80, and 90%) at the preferred orientation. Single units were sorted in Spike 2 and the output was exported to Matlab for further analysis. After initial detection of neuronal activity and potential units by an audio monitor, the threshold for spike detection was set in a way that would separate spikes from noise. The spikes were then aligned and sorted by spike 2 program based on their waveform characteristics including amplitude, slope, and trough and peak (if present). Cluster analysis and coincidence detection were further applied to determine if the quality of unit separation was satisfactory. As some units undergo a change in size after repeated firing, similar waveforms with slightly different sizes were further analyzed by coincidence detection, their receptive field, orientation selectivity and response to optogenetic silencing. A lack of overlap in the timing of spikes of the two waveforms, and a complete match for the rest would lead to combing the sorted spikes as one unit. Measurement of ocular dominance was done by presenting the above mentioned contrast stimuli to either of the eyes under light on/light off conditions. Visual stimulation and analysis scripts for electrophysiology were written in Matlab (Mathworks) and using Psychophysics Toolbox[2].

Analysis of single unit recordings and statistical comparisons

Responses were calculated as the average firing rate during visual stimulation above the spontaneous rate. Cells which did not respond with at least 2Hz to any of the visual stimuli were excluded from the analysis. For contrast and ODI measurements, only cells that preferred an orientation maximally 30 degrees different to the presented grating were included. Cells of which the firing rate increased more than 300% upon light stimulation were also omitted. Ocular dominance index was computed as ODI = (contra − ipsi response) / (contra + ipsi response). Contrast responses were fit with a Naka-Rushton curve $R0 + Rm\ contrast^n / (b^n + contrast^n)$ using Matlab's implementation of Nelder-Mead minimization. All stimulus and analysis code is available at https://github.com/heimel/InVivoTools.

Data in all groups were tested for normality using Shapiro-Wilk normality test. Parametric tests were applied if the data were either normal or became normal after square root transformation. Alternatively, nonparametric tests were applied. Significance of changes in the firing rates of individual neurons due to modulation of inhibition were assessed by Friedman test ($P<0.05$ was considered significant). Parametric and nonparametric comparisons between paired groups were done by paired t-test and Wilcoxon signed rank test, respectively. Comparisons of only two groups were performed by Student's t-test or

Mann-Whitney test. For parametric multi-comparisons of all groups with a control, Welch ANOVA (to correct for different sample sizes) followed by Dunnett's test with correction for multicomparisons were applied. For nonparametric multi-comparisons of all groups with a control, Kruskall-Wallis followed by Dunn's test with correction for multicomparisons were applied. Correlations related to in vivo whole cell recordings were calculated by Chi-square test and their P values were compared via http://www.fon.hum.uva.nl/Service/Statistics/Two_Correlations.html by using 'Fisher r-toz transformation'.

In vivo two-photon imaging of calcium signals

Animals expressing AAV-GCaMP6s specifically in PV+, SST+ or VIP+ interneurons were anesthetized with Urethane and Chlorprothixene at P33 to P37, and implanted with a glass cranial window. Two-photon calcium imaging was performed on GCaMP6s expressing neurons, using a modified Olympus BX61WI confocal microscope equipped with a Ti-sapphire laser (Mai-Tai, Spectraphysics, CA, USA), and a 20x water-immersion objective (Olympus, 0.95 NA), while presenting square wave grating stimuli. The changes in fluorescence (ΔF/F) of each neuron and specificity of the responses to orientations compared to the background were calculated using a custom Matlab script, and were used to measure orientation and direction selectivity indices.

Analysis of calcium signals

The changes in fluorescence (ΔF) of each neuron and specificity of the responses to orientations compared to the background were calculated using a custom Matlab script. Baseline fluorescence was taken as the average fluorescence from 0.5 after the offset of the previous stimulus to the start of the stimulus. Response fluorescence was calculated as the mean fluorescence from 0.5 s after stimulus onset to stimulus offset. Cells were said to be responsive if a one-sided t-test of responses versus baseline fluorescence was significant at 0.1 level.

In vivo two-photon microscopy guided cell-attached recordings

Animals injected with AAV-Arch were anesthetized with Urethane and Chlorprothixene, and, using a two-photon microscope, GFP tagged AAV-Arch expressing neurons were visualized with a 40x water immersion objective (Olympus, 0.8 NA), through a V1 craniotomy. A glass pipette (resistance 5-7MΩ) filled with a K-gluconate based internal solution (pH set to 7.3), containing 25 μM Alexa Fluor 488 hydrazide, sodium salt (Invitrogen) was inserted through the craniotomy, and, under two-photon visual guidance brought close to the target neuron. Seal was achieved by application of negative pressure. Signals were recorded in current clamp mode, filtered at 5 kHz and digitized at 10 kHz.

In vivo whole-cell recordings

Whole-cell recordings were performed as described previously [40]. In short, mice were anaesthetized with Urethane and Chlorprothixene and a patch pipette with a tip opening of ~2μm (4 - 5 MΩ), filled with a Cs+-based internal solution, pH 7.25, was inserted through the craniotomy. The evoked excitatory and inhibitory currents were recorded while clamping the cell at -70 and 0 mV, respectively. All whole-cell recordings were made from

layer 4 neurons. Excitatory and inhibitory synaptic conductances were derived according to the following equation: $\Delta I(t) = Ge(t)(V(t) - Ee) + Gi(t)(V(t) - Ei)$. $\Delta I(t)$ is the amplitude of synaptic current relative to the resting current; *Ge* and *Gi* are the excitatory and inhibitory synaptic conductance respectively; $V(t)$ is the membrane voltage, and *Ee* (0 mV) and *Ei* (-70 mV) are the reversal potentials. $V(t)$ is corrected by $V(t) = Vh - Rs*I(t)$, where *Rs* was the effective series resistance and *Vh* is the applied holding voltage. Measurement of currents at two different voltages yielded a system of two equations that could be solved for *Ge* and *Gi* at any particular *t*. Peak conductance was used to calculate the ocular dominance index (ODI).

Immunohistochemistry

Animals were perfused with 4% Paraformaldehyde (PFA) in PBS, brains were dissected out and post-fixed. 50 μm serial coronal sections, were incubated with primary antibodies to PV, SST or VIP and visualized using Alexa568. Optical sections were imaged on a Leica SP5 confocal microscope to assess localization of interneuron staining with AAV-Arch tagged GFP.

Supplementary Material

Refer to Web version on PubMed Central for supplementary material.

Acknowledgments

The authors would like to thank Emma Ruimschotel, Mehran Ahmadlou and Paul L.C. Feyen for help with experiments, drs. Vivek Jayaraman, Rex A. Kerr, Douglas S. Kim, Loren L. Looger, and Karel Svoboda from the GENIE Project, Janelia Farm Research Campus, Howard Hughes Medical Institute for providing the GCaMP6s vector, dr. Ed Boyden, MIT, Massachusetts for providing the Arch-vector, and Drs. Christian Lohmann and Rogier Min for the critical reading of the manuscript and Sophie van der Sluis for advise on statistical analyses. This research was made possible through funding from the European Community's Seventh Framework Programme (FP2007-2013) under grant agreement no 223326. This work was also funded by NWO ALW grants 823.02.001 and 821.02.002 and a grant from AgentschapNL to the Neuro-Basic PharmaPhenomics consortium. J.A.H. was supported by a VIDI grant from NWO. H.W. Tao and W.P. Ma were supported by grants from the National Institute of Health of the United States (EY019049 and EY022478).

References

1. Pouille F, Marin-Burgin A, Adesnik H, Atallah BV, Scanziani M. Input normalization by global feedforward inhibition expands cortical dynamic range. Nat. Neurosci. 2009; 12:1577–1585. [PubMed: 19881502]
2. Ozeki H, Finn IM, Schaffer ES, Miller KD, Ferster D. Inhibitory stabilization of the cortical network underlies visual surround suppression. Neuron. 2009; 62:578–592. [PubMed: 19477158]
3. Haider B, Duque A, Hasenstaub AR, McCormick DA. Neocortical network activity in vivo is generated through a dynamic balance of excitation and inhibition. J. Neurosci. 2006; 26:4535–4545. [PubMed: 16641233]
4. Higley MJ, Contreras D. Balanced excitation and inhibition determine spike timing during frequency adaptation. J. Neurosci. 2006; 26:448–457. [PubMed: 16407542]
5. Wehr M, Zador AM. Balanced inhibition underlies tuning and sharpens spike timing in auditory cortex. Nature. 2003; 426:442–446. [PubMed: 14647382]
6. Li YT, Ma WP, Li LY, Ibrahim LA, Wang SZ, Tao HW. Broadening of inhibitory tuning underlies contrast-dependent sharpening of orientation selectivity in mouse visual cortex. J. Neurosci. 2012; 32:16466–16477. [PubMed: 23152629]

7. Hensch TK, Fagiolini M, Mataga N, Stryker MP, Baekkeskov S, Kash SF. Local GABA circuit control of experience-dependent plasticity in developing visual cortex. Science. 1998; 282:1504–1508. [PubMed: 9822384]
8. Fagiolini M, Hensch TK. Inhibitory threshold for critical-period activation in primary visual cortex. Nature. 2000; 404:183–186. [PubMed: 10724170]
9. Kuhlman SJ, Olivas ND, Tring E, Ikrar T, Xu X, Trachtenberg JT. A disinhibitory microcircuit initiates critical-period plasticity in the visual cortex. Nature. 2013; 501:543–546. [PubMed: 23975100]
10. van Versendaal D, Rajendran R, Saiepour MH, Klooster J, Smit-Rigter L, Sommeijer JP, De Zeeuw CI, Hofer SB, Heimel JA, Levelt CN. Elimination of inhibitory synapses is a major component of adult ocular dominance plasticity. Neuron. 2012; 74:374–383. [PubMed: 22542189]
11. Chen JL, Villa KL, Cha JW, So PT, Kubota Y, Nedivi E. Clustered dynamics of inhibitory synapses and dendritic spines in the adult neocortex. Neuron. 2012; 74:361–373. [PubMed: 22542188]
12. Donato F, Rompani SB, Caroni P. Parvalbumin-expressing basket-cell network plasticity induced by experience regulates adult learning. Nature. 2013; 504:272–276. [PubMed: 24336286]
13. Froemke RC, Merzenich MM, Schreiner CE. A synaptic memory trace for cortical receptive field plasticity. Nature. 2007; 450:425–429. [PubMed: 18004384]
14. Chittajallu R, Isaac JT. Emergence of cortical inhibition by coordinated sensory-driven plasticity at distinct synaptic loci. Nat. Neurosci. 2010; 13:1240–1248. [PubMed: 20871602]
15. Sillito AM, Kemp JA, Blakemore C. The role of GABAergic inhibition in the cortical effects of monocular deprivation. Nature. 1981; 291:318–320. [PubMed: 7231550]
16. Duffy FH, Burchfiel JL, Conway JL. Bicuculline reversal of deprivation amblyopia in the cat. Nature. 1976; 260:256–257. [PubMed: 1256565]
17. Yazaki-Sugiyama Y, Kang S, Cateau H, Fukai T, Hensch TK. Bidirectional plasticity in fast-spiking GABA circuits by visual experience. Nature. 2009; 462:218–221. [PubMed: 19907494]
18. Zheng W, Knudsen EI. Functional selection of adaptive auditory space map by GABAA-mediated inhibition. Science. 1999; 284:962–965. [PubMed: 10320376]
19. Hubel DH, Wiesel TN, LeVay S. Plasticity of ocular dominance columns in monkey striate cortex. Philos. Trans. R. Soc. Lond B Biol. Sci. 1977; 278:377–409. [PubMed: 19791]
20. Maffei A, Nataraj K, Nelson SB, Turrigiano GG. Potentiation of cortical inhibition by visual deprivation. Nature. 2006; 443:81–84. [PubMed: 16929304]
21. Maffei A, Nelson SB, Turrigiano GG. Selective reconfiguration of layer 4 visual cortical circuitry by visual deprivation. Nat. Neurosci. 2004; 7:1353–1359. [PubMed: 15543139]
22. Smith GB, Bear MF. Bidirectional ocular dominance plasticity of inhibitory networks: recent advances and unresolved questions. Front Cell Neurosci. 2010; 4:21. [PubMed: 20592959]
23. Gandhi SP, Yanagawa Y, Stryker MP. Delayed plasticity of inhibitory neurons in developing visual cortex. Proc. Natl. Acad. Sci. U. S. A. 2008; 105:16797–16802. [PubMed: 18940923]
24. Kameyama K, Sohya K, Ebina T, Fukuda A, Yanagawa Y, Tsumoto T. Difference in binocularity and ocular dominance plasticity between GABAergic and excitatory cortical neurons. J. Neurosci. 2010; 30:1551–1559. [PubMed: 20107082]
25. Chow BY, Han X, Dobry AS, Qian X, Chuong AS, Li M, Henninger MA, Belfort GM, Lin Y, Monahan PE, et al. High-performance genetically targetable optical neural silencing by light-driven proton pumps. Nature. 2010; 463:98–102. [PubMed: 20054397]
26. Atallah BV, Bruns W, Carandini M, Scanziani M. Parvalbumin-expressing interneurons linearly transform cortical responses to visual stimuli. Neuron. 2012; 73:159–170. [PubMed: 22243754]
27. Atallah BV, Scanziani M, Carandini M. Atallah et al. reply. Nature. 2014; 508:E3. [PubMed: 24695314]
28. Lee SH, Kwan AC, Dan Y. Interneuron subtypes and orientation tuning. Nature. 2014; 508:E1–E2. [PubMed: 24695313]
29. El-Boustani S, Wilson NR, Runyan CA, Sur M. El-Boustani et al. reply. Nature. 2014; 508:E3–E4. [PubMed: 24695315]

30. Lee SH, Kwan AC, Zhang S, Phoumthipphavong V, Flannery JG, Masmanidis SC, Taniguchi H, Huang ZJ, Zhang F, Boyden ES, et al. Activation of specific interneurons improves V1 feature selectivity and visual perception. Nature. 2012; 488:379–383. [PubMed: 22878719]
31. Wilson NR, Runyan CA, Wang FL, Sur M. Division and subtraction by distinct cortical inhibitory networks in vivo. Nature. 2012; 488:343–348. [PubMed: 22878717]
32. Chen TW, Wardill TJ, Sun Y, Pulver SR, Renninger SL, Baohan A, Schreiter ER, Kerr RA, Orger MB, Jayaraman V, et al. Ultrasensitive fluorescent proteins for imaging neuronal activity. Nature. 2013; 499:295–300. [PubMed: 23868258]
33. Adesnik H, Bruns W, Taniguchi H, Huang ZJ, Scanziani M. A neural circuit for spatial summation in visual cortex. Nature. 2012; 490:226–231. [PubMed: 23060193]
34. Fu Y, Tucciarone JM, Espinosa JS, Sheng N, Darcy DP, Nicoll RA, Huang ZJ, Stryker MP. A cortical circuit for gain control by behavioral state. Cell. 2014; 156:1139–1152. [PubMed: 24630718]
35. Khibnik LA, Cho KK, Bear MF. Relative contribution of feedforward excitatory connections to expression of ocular dominance plasticity in layer 4 of visual cortex. Neuron. 2010; 66:493–500. [PubMed: 20510854]
36. Ma WP, Li YT, Tao HW. Downregulation of cortical inhibition mediates ocular dominance plasticity during the critical period. J. Neurosci. 2013; 33:11276–11280. [PubMed: 23825430]
37. Iurilli G, Olcese U, Medini P. Preserved Excitatory-Inhibitory Balance of Cortical Synaptic Inputs following Deprived Eye Stimulation after a Saturating Period of Monocular Deprivation in Rats. PLoS. One. 2013; 8:e82044. [PubMed: 24349181]
38. Pouille F, Scanziani M. Enforcement of temporal fidelity in pyramidal cells by somatic feed-forward inhibition. Science. 2001; 293:1159–1163. [PubMed: 11498596]
39. Fries P, Nikolic D, Singer W. The gamma cycle. Trends Neurosci. 2007; 30:309–316. [PubMed: 17555828]
40. Ma WP, Liu BH, Li YT, Huang ZJ, Zhang LI, Tao HW. Visual representations by cortical somatostatin inhibitory neurons--selective but with weak and delayed responses. J. Neurosci. 2010; 30:14371–14379. [PubMed: 20980594]
41. Wang Y, Toledo-Rodriguez M, Gupta A, Wu C, Silberberg G, Luo J, Markram H. Anatomical, physiological and molecular properties of Martinotti cells in the somatosensory cortex of the juvenile rat. J. Physiol. 2004; 561:65–90. [PubMed: 15331670]
42. Cruikshank SJ, Ahmed OJ, Stevens TR, Patrick SL, Gonzalez AN, Elmaleh M, Connors BW. Thalamic control of layer 1 circuits in prefrontal cortex. J. Neurosci. 2012; 32:17813–17823. [PubMed: 23223300]
43. Zhang S, Xu M, Kamigaki T, Hoang Do JP, Chang WC, Jenvay S, Miyamichi K, Luo L, Dan Y. Selective attention. Long-range and local circuits for top-down modulation of visual cortex processing. Science. 2014; 345:660–665. [PubMed: 25104383]
44. Pfeffer CK, Xue M, He M, Huang ZJ, Scanziani M. Inhibition of inhibition in visual cortex: the logic of connections between molecularly distinct interneurons. Nat. Neurosci. 2013; 16:1068–1076. [PubMed: 23817549]
45. Alitto HJ, Dan Y. Cell-type-specific modulation of neocortical activity by basal forebrain input. Front Syst. Neurosci. 2012; 6:79. [PubMed: 23316142]
46. Kaneko M, Stryker MP. Sensory experience during locomotion promotes recovery of function in adult visual cortex. Elife. 2014; 3:e02798. [PubMed: 24970838]
47. Toyoizumi T, Miyamoto H, Yazaki-Sugiyama Y, Atapour N, Hensch TK, Miller KD. A theory of the transition to critical period plasticity: inhibition selectively suppresses spontaneous activity. Neuron. 2013; 80:51–63. [PubMed: 24094102]

Highlights

- Inhibition in visual cortex is predominantly provided by parvalbumin interneurons
- In individual neurons, inhibitory and excitatory inputs from both eyes are balanced
- Ocular dominance plasticity disrupts binocularly matched inhibition and excitation
- Ocular dominance plasticity is not driven by eye-specific changes in inhibition

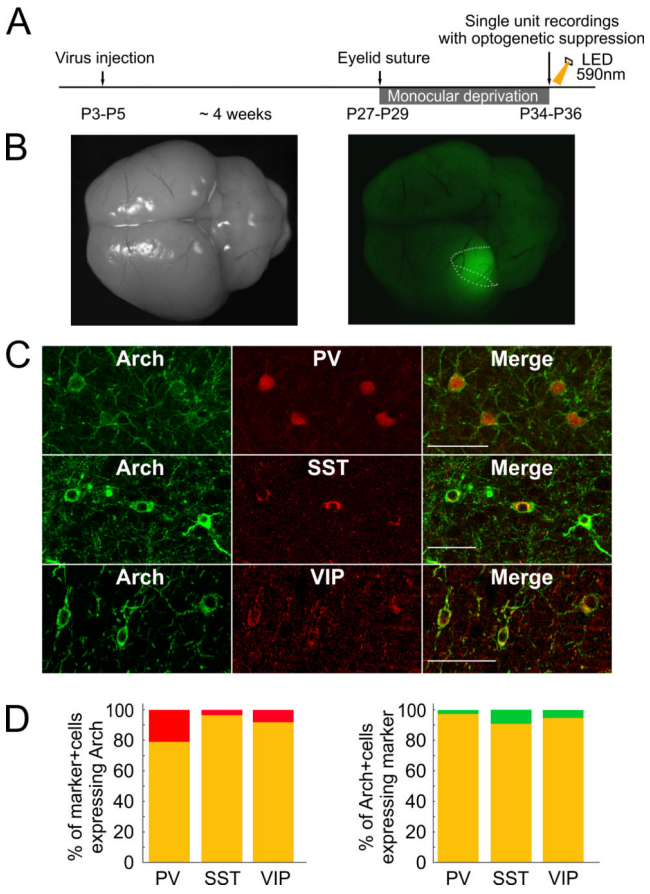

Figure 1. Experimental timeline and quantitation of Archaerhodopsin expression in interneuron subtypes

(**A**) Experimental timeline. Animals were monocularly deprived for 7 days, or were not subjected to deprivation. In some cases mice were deprived for only 1 or 3-4 days. P: postnatal day. (**B**) Whole brain view in brightfield (left) and fluorescence (right) showing extent of archaerhodopsin-GFP (Arch-GFP) expression. Dotted lines indicate rough outline of V1, with binocular region marked separately. (**C**) Co-expression of Arch-GFP in parvalbumin- (PV)-, somatostatin (SST)- and vasoactive intestinal peptide- (VIP)-cre mice with the corresponding interneuron markers. Scale bar = 50 μm (**D**) Percentage of neurons positive for PV (79%), SST (94%) or VIP (92%) co-expressing Arch (left) and percentage of Arch expressing neurons co-expressing PV (97%), SST (91%) or VIP (95%) (right).

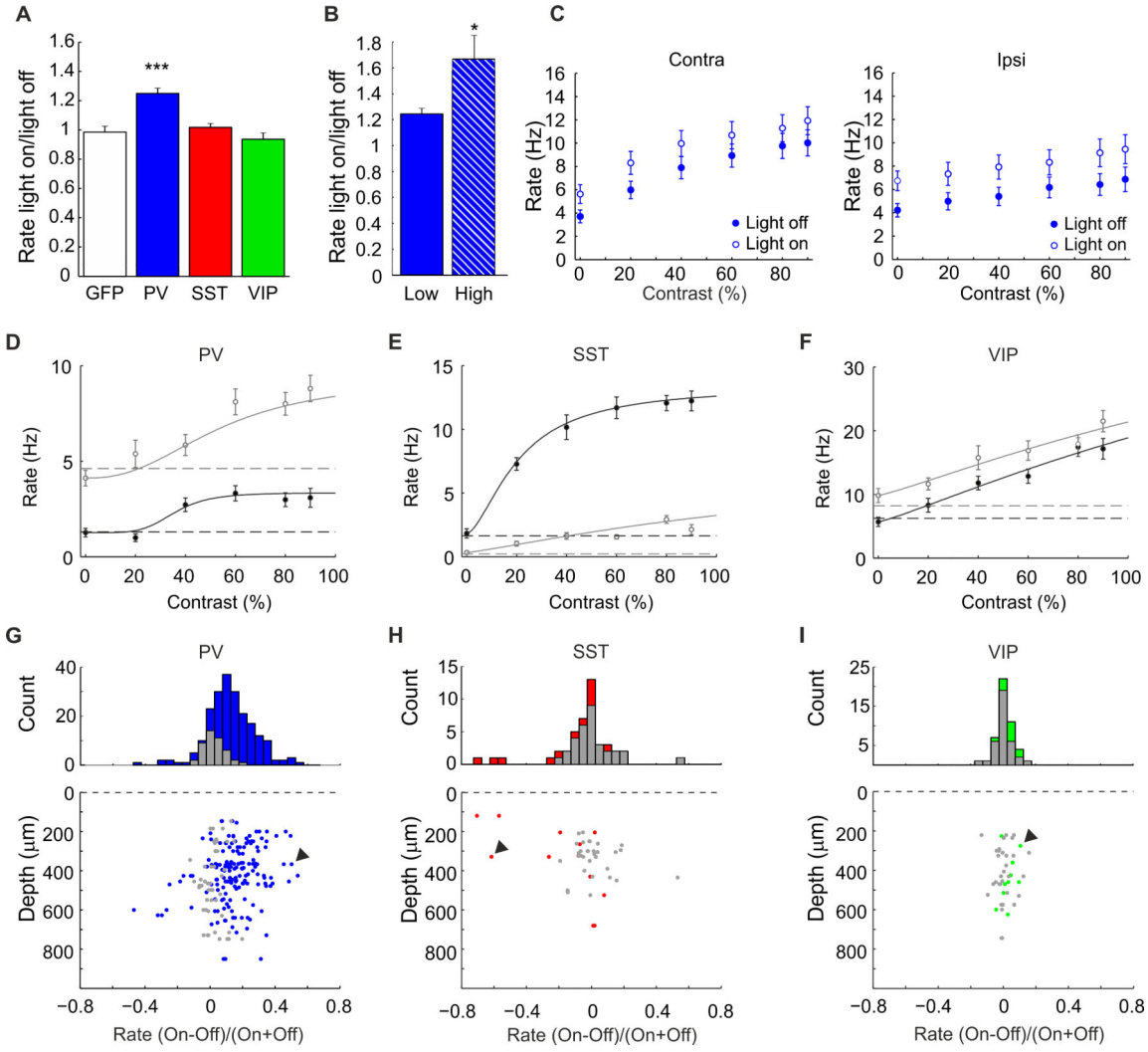

Figure 2. Suppression of archaerhodopsin-expressing interneurons with light

(**A**) Normalized average response rates upon illuminating PV+ interneurons expressing GFP or PV+, SST+ or VIP+ interneurons expressing Arch. (**B**) Illuminating PV+ interneurons expressing Arch with 1.5-5 mW does not saturate responses as they are increased further by 5-9 mW light (High). (**C**) Average contralateral- and ipsilateral-eye contrast response curves do not show saturation when PV+ interneurons are optogenetically suppressed. (**D-F**) Sample contrast-response curves of single units upon suppression if PV+ (**D**), SST+ (**E**) or VIP+ (**F**) interneurons. Black and grey lines depict fitting curves for non-suppressed and suppressed conditions, respectively. Horizontal black and grey dashed lines represent spontaneous rates for light off and light on conditions, respectively. (**G-I**) Changes in firing rate of single units at different depths in suppressed versus non-suppressed conditions, shown as a histogram (top) and dot plot (bottom) for mice expressing Arch in PV+ (**G**), SST + (**H**) and VIP+ (**I**) interneurons. Color represents neurons whose contrast-response curve is significantly altered (Friedman, $p<0.05$) while grey represents neurons whose responses are not significantly altered. * $p<0.05$, *** $p<0.001$. Arrowheads indicate neurons whose contrast-response curves are shown in **D-F**. Results expressed as mean ± SEM.

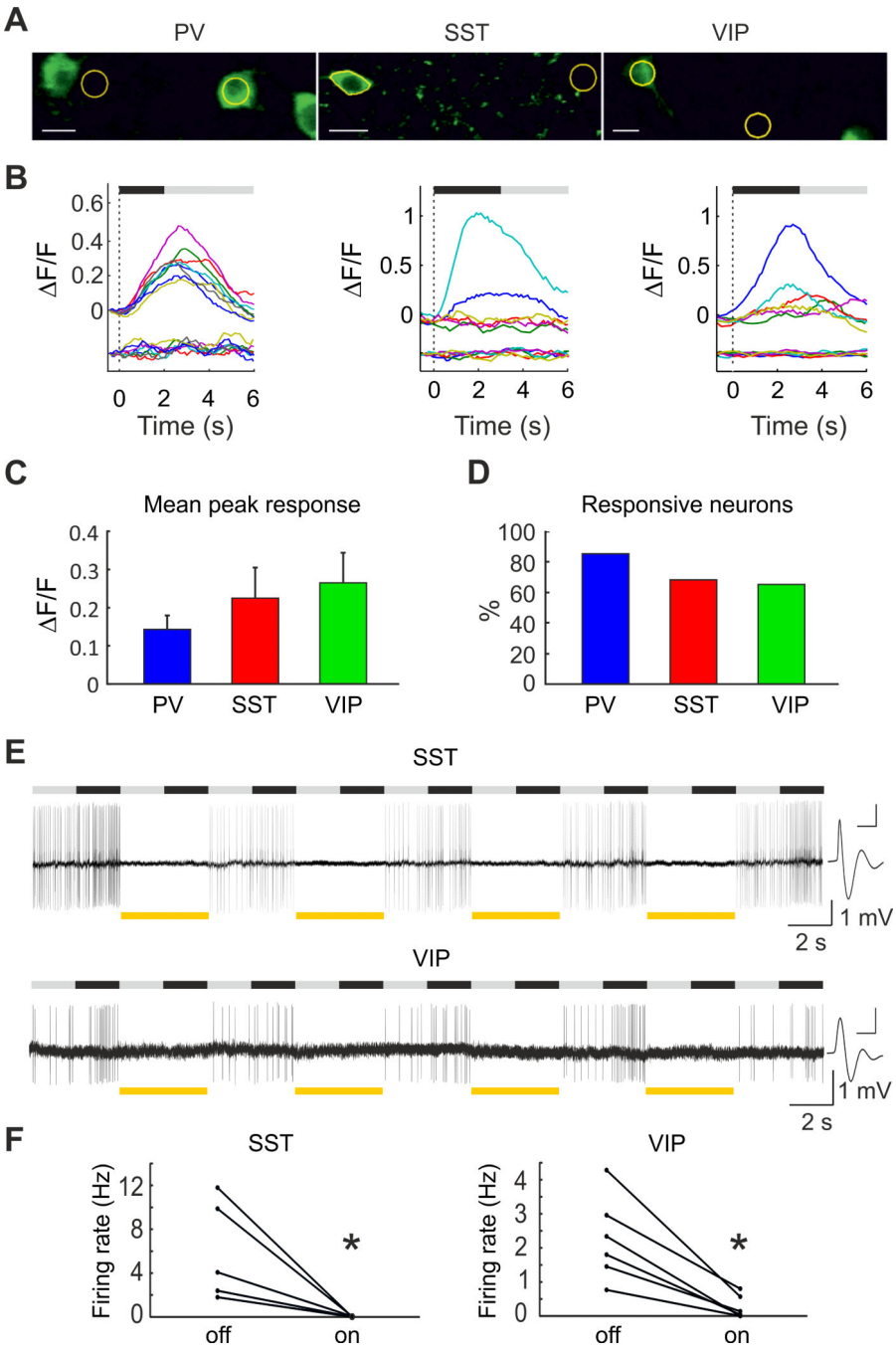

Figure 3. PV+, SST+ and VIP+ interneurons are visually responsive and can be optogenetically suppressed

(**A**) Representative images showing ROIs (yellow outlines) used for analysis of calcium responses for PV+, SST+ and VIP+ interneurons and respective neuropil. Scale bars are 10μm. (**B**) Average traces of calcium transients of representative PV+, SST+ and VIP+ interneurons (top) and neuropil (bottom) as assessed by *in vivo* two-photon calcium imaging using GCaMP6s. The different colors of the traces represent average ΔF/F curves of different orientations, while grey and black bars at the top represent the presentation of a grey screen and visual stimulus, respectively. Y-axis of neuropil traces have been scaled to

match neuronal traces. (**C**) Mean peak response of PV+, SST+ and VIP+ interneurons. (**D**) Percentage of PV+, SST+ and VIP+ interneurons neurons responsive to visual stimuli. (**E**) *In vivo* two-photon guided cell-attached recordings of an SST+ and a VIP+ interneuron expressing Arch. Grey and black bars above the trace represent the presentation of a grey screen and visual stimulus, respectively. Yellow boxes represent light on epochs. Neuronal activity is increased during visual stimulation, and silenced during amber light illumination. Average spike waveform of SST+ and VIP+ interneurons, scale bars represent 4ms and 1 mV. (F) Optogenetic suppression of SST+, and VIP+ interneurons. Firing rates are average responses to a grey screen and visual stimuli. Results expressed as mean +/− SEM. * $P<0.05$.

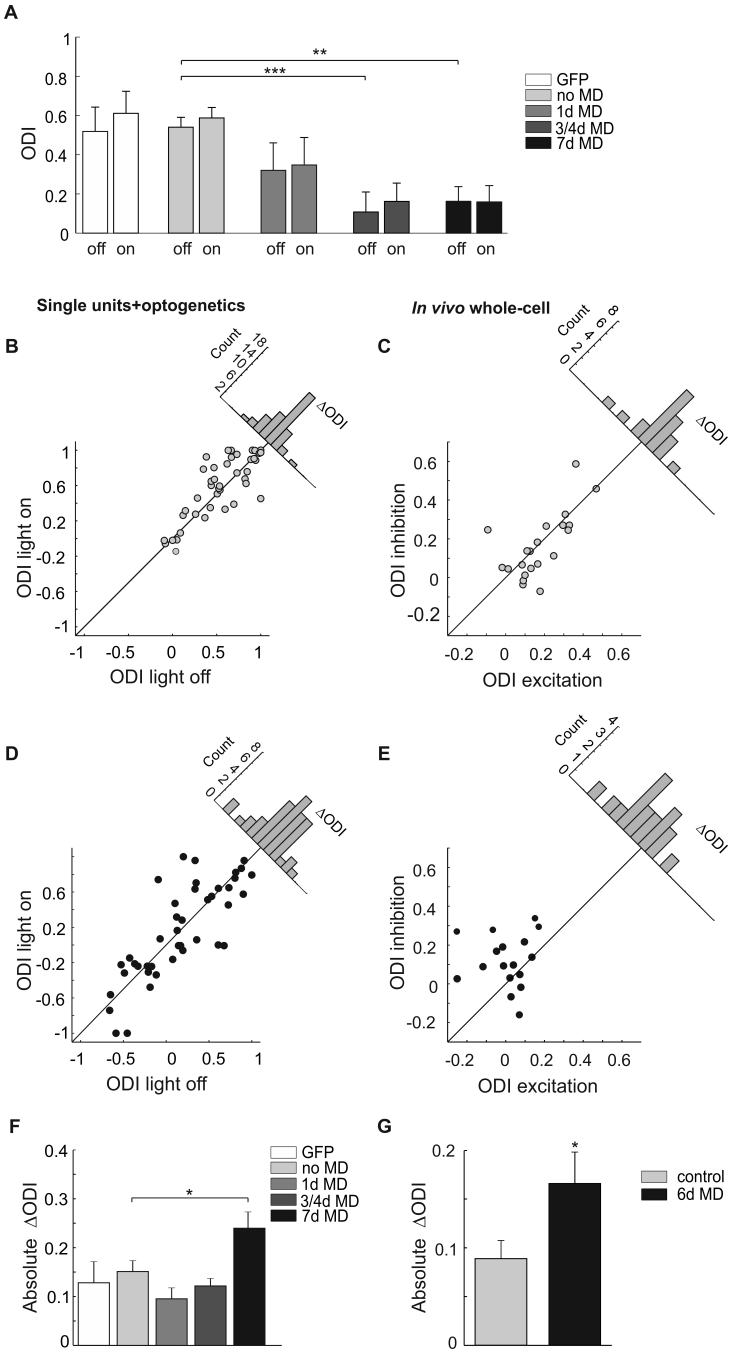

Figure 4. Effects of inhibitory input and monocular deprivation on ocular dominance

(**A**) Average ocular dominance index (ODI) values are not altered by PV+ interneuron suppression in controls or monocularly deprived littermates. (**B, D**) Scatter plots of ODIs of single units under light on vs light off conditions in non-deprived (**B**) and 7 day monocularly deprived littermates (**D**). (**C, E**) Scatter plots of ODIs of inhibitory vs excitatory inputs assessed by *in vivo* whole cell recordings in controls (**C,** figure adapted from Ma et al, 2013) and 6 day monocularly deprived littermates (**E**). Distribution histograms are shown on top right of the scatter plots (**B-E**). (**F**) Absolute difference in ODIs of single units under light

off and light on conditions in control and monocularly deprived mice. (**G**) Absolute difference in ODIs of inhibitory and excitatory inputs in control and monocularly deprived mice. * $p<0.05$, ** $p<0.01$, *** $p<0.001$. Error bars represent SEM.